A Hybrid ECEEMDAN-LGBM Framework for Knee Joint Vibroarthrographic Signal Classification

Krishna Sundeep Basavaraju
National Institute of Technology Warangal, India
bs721065@studen.nitw.ac.in (corresponding author)

T. Kishore Kumar
National Institute of Technology Warangal, India
kishoret@nitw.ac.in

K. Ashoka Reddy
Kakatiya Institute of Technology & Science, Warangal, India
kareddy.iitm@gmail.com

Received: 30 December 2025 | Revised: 26 January 2026 | Accepted: 7 February 2026

 DOI: https://doi.org/10.48084/etasr.17260

ABSTRACT

The significance of early diagnosis and adaptability to non-invasive procedures for detecting knee disorders has become very prominent. Vibroarthrography is one of the prominent non-invasive methods that uses signals produced during the movement of the knee joint to assess its degradation. This study presents a comprehensive approach that combines Enhanced Complete Ensemble Empirical Mode Decomposition with Adaptive Noise (ECEEMDAN) for signal decomposition and the Light Gradient Boosting Machine (LGBM) classifier for the analysis and classification of Vibroarthrographic (VAG) signals. The proposed approach focuses on identifying the significant frequency components by decomposing these vibration signals into Intrinsic Mode Functions (IMFs), followed by a novel energy-correlation-kurtosis-based adaptive IMF selection strategy for effective signal reconstruction. Entropy features, such as Approximate Entropy (*ApEn*), Sample Entropy (*SampEn*), and Shannon Entropy (*ShEn*), are extracted for the reconstructed signals and the decomposed sub-bands. Several machine learning classifiers, such as Decision Tree (DT), XGBoost (XGB), Gradient Boosting (GB), Random Forest (RF), SVM, and Light Gradient Boosting Machines (LGBM), are used for classification. Based on test results, the LGBM classifier achieved good levels of accuracy at 90.56%, AUROC at 0.9120, sensitivity at 92.10%, specificity at 90.23%, positive predictive value at 87.56%, and negative predictive value at 93.95%.

Keywords-Vibroarthrographic (VAG) signals; empirical mode decomposition; Intrinsic Mode Functions (IMFs); entropy features; Light Gradient Boosting Machine (LGBM) classifier

I. INTRODUCTION

Articular Cartilage (AC) plays a vital role in the biomechanics of synovial joints, easing motion and leading to minimal friction during load transfer. Its biomechanical behavior, governed by a complex structure of type II collagen, proteoglycans, and water, provides elasticity, viscoelastic stress relaxation, and anisotropic response under cyclic loading. These properties deteriorate with aging, mechanical overload, and degenerative conditions such as Osteoarthritis (OA), leading to progressive joint dysfunction [1]. Many factors, such as occupational loading, sports activity, prior injuries, obesity, and sex-related biomechanical differences, can influence the progression of OA [1-3]. Current diagnosis methods are helpful in mainly alleviating symptoms and do not reverse cartilage degeneration, highlighting the need for early detection [2]. However, early-stage OA remains difficult to diagnose clinically, while conventional imaging methods are costly, invasive, or unsuitable for routine screening [2, 3]. Due to these factors, attention has been shifted toward Vibroarthrography (VAG) and kinematic motion analysis as non-invasive alternatives for assessing joint function through movement-induced vibroacoustic signals.

Several VAG-based methods have been proposed to investigate knee joint disorders. In [4, 5], parametric representation methods were introduced for knee screening using VAG signals, demonstrating their efficacy in separating pathological from normal joints. In [6], time and spectral domain features in VAG-based knee screening were compared,

with a focus on the significance of feature extraction algorithms to improve classification accuracy. In [7], the investigation was extended to entropy-based metrics to measure knee VAG signal abnormalities related to cartilage disease. In [8], the Tunable Q-Factor Wavelet Transform (TQWT) was used to classify VAG signals, demonstrating its versatility in feature extraction.

In [9], a novel actigraphy-based VAG signal analysis system was presented to help assess the severity of knee cartilage degradation, achieving an accuracy of 84.6%. In [10], knee degradation was assessed using high-frequency features from VAG signals, achieving a good specificity of 0.8 and a sensitivity of 0.75 using an SVM classifier. In [11], three logistic regression techniques were used to assess cartilage degradation using the VAG signals by employing 72 extracted features, achieving an accuracy of 84%. In [12], improved sensor placement for VAG signal acquisition was investigated, considering various movement conditions. In [13], statistical features and spectral features were used from VAG signals, achieving a classification accuracy of 89.23%.

Regarding more recent studies, in [14], VAG was improved by transforming signals into the angle domain using goniometer-based resampling and dynamic time warping, enhancing interpretability and reducing motion-related nonlinearity. This study further demonstrated that VAG features vary continuously with external load, confirming VAG's sensitivity to knee joint arthrokinematics and load-dependent mechanics [15]. The study in [16] extensively demonstrated the potential of VAG and motion-based sensing for non-invasive knee osteoarthritis assessment. A series of studies [17-19] showed that carefully selected vibroacoustic and kinematic features, combined with machine learning models such as MLP, RBF, SVM, and ANN-based frameworks, can reliably distinguish healthy and osteoarthritic knees with high accuracy, sensitivity, and specificity. Acoustic signal discriminants, advanced signal analysis techniques (EEMD-DFA, recurrence quantification), and wearable encoder-based motion analysis collectively highlight the clinical promise of data-driven approaches for early functional diagnosis beyond conventional imaging [20, 21].

Our previous work [22] on the analysis of VAG signals using the Empirical Wavelet Transform method and statistical features achieved an accuracy of 83.3%, while our next work [23] used TQWT and entropy measures to achieve an accuracy of 87%. This work aimed to investigate VAG signals using an adaptive framework. This study hypothesized that feature-guided IMF selection based on adaptive ECEEMDAN decomposition can improve diagnostic performance, with the novelty arising from its integration with a Light Gradient Boosting Machine (LGBM) compared to existing CEEMDAN-based approaches.

II. METHODOLOGY

Figure 1 shows the proposed framework for knee abnormality classification, which involves: (i) Preprocessing, (ii) Decomposition using EMD, (iii) Selection of IMFs, (iv) Signal reconstruction, (v) Feature extraction, and (vi) classification.

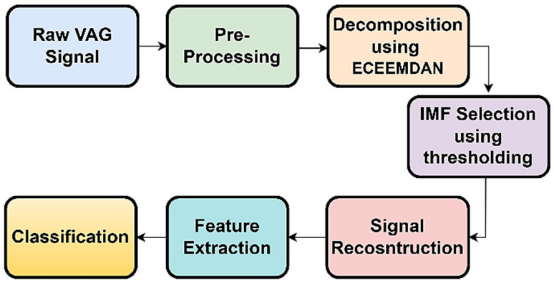

Fig. 1. VAG signal analysis workflow.

A. Preprocessing of VAG Signals

This study used VAG signals from [4], while its subsequent use and validation for knee joint assessment are reported in [5]. This technique yielded 89 VAG recordings in total.

TABLE I. DATASET DETAILS [4, 5]

Class	No. of Participants	Age (Mean ± SD, years)	Males:Females
Normal	51	28 ± 9.54	22 : 29
Abnormal	38	35 ± 13.89	20 : 18

To record the vibrations caused by the knee's movement, a miniature accelerometer (Model 3115A, Dytran Instruments, USA) was placed at the center of the patella. Subjects were seated with their legs freely suspended and performed controlled knee extension-flexion movements from 135° to 0° within 4 s. The signals were recorded at a sampling rate of 2 kHz, bandpass filtered (10 Hz–1 kHz), amplified, and digitized with 12-bit resolution using a National Instruments data acquisition system. These signals were preprocessed using a cascading moving average filter [24]. Figure 2 shows the VAG signals that correlate with normal and pathological knee joint states.

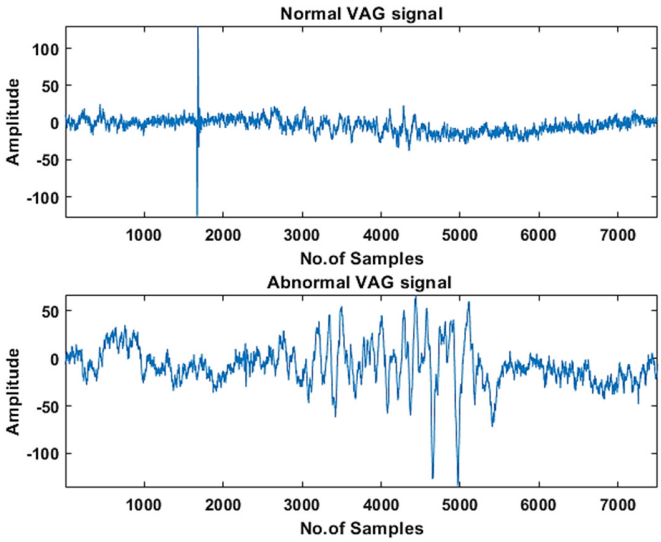

Fig. 2. VAG signals: Normal and Abnormal

B. Decomposition of VAG Signals

ECEEMDAN [25] was implemented for decomposing the VAG signals. This approach, instead of adding fixed white noise across the entire signal, dynamically generates noise based on local variability in the signal. This ensures that the added noise better reflects the signal's non-stationary nature and helps reduce mode mixing during decomposition. It begins by sliding a window of size n across the normalized input signal x. For each windowed segment, the local mean μ_i is calculated, along with the local standard deviation SD_i. These values capture how much the signal is fluctuating in that specific segment, rather than using a single global value for the entire signal:

$$\mu_i = \frac{1}{n}\sum_{j=1}^{i+n-1} x_j \quad (1)$$

$$SD_i = \sqrt{\frac{\sum_{j=1}^{i+n-1}(x_j-\mu_i)^2}{n}} \quad (2)$$

Next, white Gaussian noise is generated, which matches the local variability. For each realization (from $i = 1$ to NR):

- A random noise vector is drawn from a standard uniform distribution R(0, 1)
- It is scaled using the local SD_i and a tuning parameter β_i
- Finally, this scaled noise is added to the original signal:

$$x^{(i)} = x + R(0,1) * SD_i * \beta_i \quad (3)$$

Each noisy signal $x^{(i)}$ is decomposed using EMD to extract the first mode d_1 and its residual r_1. The ensemble average is computed across all realizations to obtain a more stable result:

$$r_1 = \langle M(x^{(i)}) \rangle \quad (4)$$

Then, an auxiliary mean is calculated using:

$$aux = \frac{(x^{(i)}-d_1)}{NR} \quad (5)$$

This represents the remaining signal content after removing the first mode. This residual is further decomposed until no more meaningful modes can be extracted or until a stopping condition is met. After each mode is extracted:

- The auxiliary mean is updated,
- Noise is added again,
- Decomposition continues on the updated signal.

Each noisy signal is also smoothed using a Savitzky-Golay filter to minimize artifacts:

$$\hat{y}_i = \sum_{j=-n}^{n} C_j x^{(i+j)} \quad (6)$$

After all realizations are processed, the standard deviation of the difference between the noisy signal and the extracted IMFs is calculated:

$$SDN_i = \sqrt{\frac{\sum((x^{(i)}-IMF_i)-\mu)^2}{n}} \quad (7)$$

Then, the noise is generated adaptively using:

$$w^{(i)} = \beta_i * SDN_i * R(0,1) \quad (8)$$

The ensemble size (NR) determines the number of noise-assisted realizations and was set to 100 to ensure stable mode estimation. The window size is adaptively computed from the signal autocorrelation, dominant frequency, and noise level, allowing dynamic adjustment to signal characteristics. The noise amplitude β is automatically estimated using spectral entropy, SNR, and local variability, providing adaptive noise injection and improved mode separation. Figure 3 shows the VAG signal decomposed using ECEEMDAN.

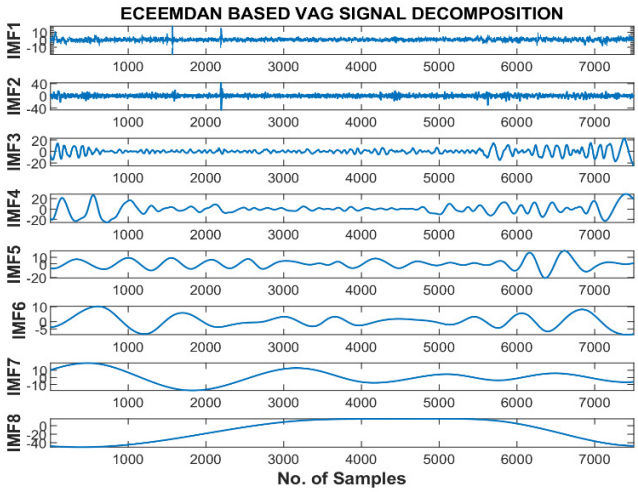

Fig. 3. VAG signal decomposed using ECEEMDAN.

C. Selection of IMFs

This work introduces an adaptive system for knee joint abnormality classification using VAG signals. Starting with the raw signals, the proposed method extracts the IMFs that accurately reflect the frequency and amplitude fluctuations needed for a proper diagnosis, after which the most significant IMFs are intelligently chosen utilizing techniques such as EMD, EEMD, CEEMDAN, and ECEEMDAN [25-28], in combination with LGBM.

1) Feature Extraction from IMFs

Once the signals are decomposed, three key features are calculated for each IMF:

- Energy ($E_{k,i}$) represents the signal's energy within the IMF and reflects its strength.
- Correlation ($\rho_{k,i}$) is used to determine the degree to which the IMF is similar to the original signal.
- Kurtosis ($K_{k,i}$) indicates the "peakiness" of the IMF and helps identify sharp, impulsive events, which are often important in medical signal analysis, where k =1, 2, …, 89 and i indicates the IMF. Each IMF's features are stored, with each IMF assigned the class label of its corresponding signal (e.g., normal or diseased) $[E_{k,i}, \rho_{k,i}, K_{k,i}]$.

2) Determining Feature Importance with LGBM

After extracting features, the model is trained, and feature significance scores are calculated. For each VAG signal, IMFs are ranked by their scores, and those exceeding the mean of all IMF scores computed for that same signal are selected for reconstruction. The score for each IMF is given by:

$$S_i = w_1 \cdot E_i + w_2 \cdot C_i + w_3 \cdot K_i \quad (9)$$

Figure 4 shows the reconstructed signal for all EMD variants using the above thresholds. Algorithm 1 shows a pseudo-code that describes the proposed method.

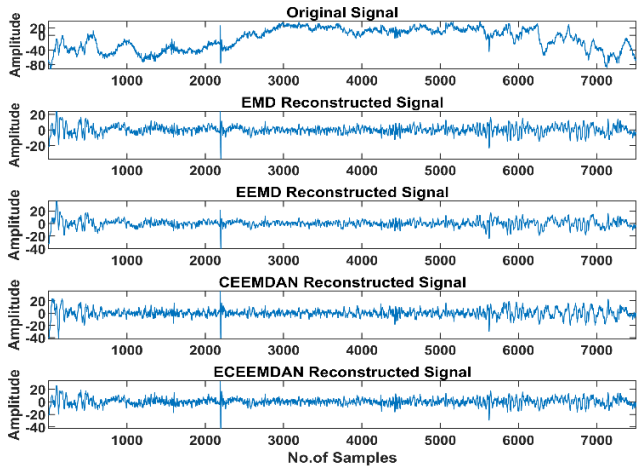

Fig. 4. VAG signal reconstructed from the selected IMFs.

Input: Signal $x \in \mathbb{R}^n$, number of IMFs N
Output:
Selected IMFs, Feature importance weights $[w_1, w_2, w_3]$, reconstructed signal
1. Decompose signal:
Apply ECEEMDAN to obtain N IMFs:
IMFs = ECEEMDAN(x, N)
2. Extract features for each IMF $i = 1$ to N:
Energy: $E_i = \sum IMF_i[j]^2$
Correlation: $C_i = corr(IMF_i, x)$
Kurtosis: $K_i = kurtosis(IMF_i)$
3. Construct feature matrix:
$F = [E_i, C_i, K_i] \in \mathbb{R}^{N \times 3}$
4. Define pseudo-target for unsupervised regression:
$y_i = E_i C_i$ (for all $i = 1, \ldots, N$)
5. Train LGBM regressor
Train an LGBM model using F as input and y as target.
6. Extract and normalize feature importances:
Let g_E, g_C, g_K be gain-based importances for energy, correlation, and kurtosis.
Normalize weights:
$w_1 = g_E/(g_E + g_C + g_K)$
$w_2 = g_C/(g_E + g_C + g_K)$
$w_3 = g_K/(g_E + g_C + g_K)$
7. Score each IMF:
$S_i = w_1 \cdot E_i + w_2 \cdot C_i + w_3 \cdot K_i$
8. Select relevant IMFs:
Rank IMFs based on S_i in descending order.
Select the top K IMFs that cross the mean score.
9. Reconstruct the signal:
$\hat{x} = \sum IMF_i$ selected based on threshold
10. Return:
IMFs, feature weights $[w_1, w_2, w_3]$, and reconstructed signal $\hat{x}$

D. Feature Extraction

The following entropy features were calculated from the sub-bands and reconstructed VAG signals.

- Approximate Entropy: Estimates the amount of regularity of data [29]

$$ApEN = \phi^m(r) - \phi^{m+1}(r) \quad (10)$$

where

$$\phi^m(r) = (N - m + 1)^{-1} \sum_{i=1}^{N-m+1} log\,(c_i^m(r)) \quad (11)$$

Here r is the filtering level, m is the window length, and ϕ are patterns estimated of particular length.

- Sample Entropy: Assess the amount of regularity of data [30]

$$SampEn = -ln\frac{A}{B} \quad (12)$$

where A is the number of template vector pairs satisfying:

$d[Xm + 1\,(i), Xm + 1\,(j)] < r$

B is the number of template vector pairs satisfying:

$d[Xm(i), Xm\,(j)] < r$

m is the embedding dimension, and r is the tolerance.

- Shannon Entropy: Estimates the uncertainty of the random process [31]:

$$H = -\frac{1}{log\,N} \sum_i p_i \log(p_i) \quad (13)$$

where H represents the entropy, p_i denotes the probability of the i^{th} event, and N is the total number of possible states. The entropy parameters were set to m= 2 and $r = 0.2 \times SD$, following established biomedical signal analysis practice. A brief sensitivity analysis confirmed that this configuration provides stable entropy estimates and consistent classification performance. For m = 1 and m = 3, varying r within $0.1 - 0.3 \times SD$ did not yield stable or discriminative entropy features; hence, only the optimal configuration (m=2, $r = 0.2 \times SD$) is reported.

E. Classification

Applying the LGBM classifier to a dataset of VAG signals allowed us to differentiate between normal and pathological VAG signals. Common metrics include the Area Under the Receiver Operating Characteristic Curve (AUROC), sensitivity, specificity, accuracy, and positive and negative predictive values. These metrics help assess how effectively the method distinguishes between the two signal categories. This study evaluated the LGBM classifier in several EMD variant decompositions [25-28] alongside other popular machine learning models, including DT, RF, GB, XGB, and a regular SVM. A 10-fold stratified cross-validation strategy was employed to ensure robust and reproducible performance evaluation.

III. RESULTS

As shown in Tables II-V, LGBM consistently performed better than the other classifiers across all decomposition methods. Using EMD, LGBM achieved an accuracy of 83.14% (AUROC = 0.8316), which improved to 86.47% (AUROC = 0.8666) with EEMD and 87.58% (AUROC = 0.8732) with CEEMDAN. The proposed ECEEMDAN-based framework produced the best overall results, with LGBM achieving the highest accuracy of 90.56% and an AUROC of 0.9120, along with strong sensitivity (92.10%) and specificity (90.23%), indicating superior discrimination of knee joint abnormalities. Using EMD features, LGBM achieved an accuracy of 83.14% (AUROC = 0.8316), which improved to 86.47% (AUROC = 0.8666) with EEMD and 87.58% (AUROC = 0.8732) with CEEMDAN, while SVM generally yielded the lowest performance.

TABLE II. CLASSIFICATION RESULTS OF EMD

Model	ACC	SEN	SPEC	PPV	NPV	AUROC
LGBM	0.8314	0.8214	0.8418	0.8007	0.8709	0.8316
XGB	0.8203	0.8214	0.8218	0.7864	0.8753	0.8216
GB	0.8078	0.7643	0.8400	0.8019	0.8410	0.8021
RF	0.8039	0.8071	0.8018	0.7448	0.7740	0.8045
SVM	0.7941	0.7571	0.8218	0.7583	0.7458	0.7895

TABLE III. CLASSIFICATION RESULTS OF EEMD

Model	ACC	SEN	SPEC	PPV	NPV	AUROC
LGBM	0.8647	0.8714	0.8618	0.8569	0.9175	0.8666
XGB	0.8431	0.7893	0.8836	0.8543	0.8543	0.8365
GB	0.8529	0.8214	0.8800	0.8873	0.8910	0.8507
RF	0.8209	0.7679	0.8655	0.8143	0.8351	0.8167
SVM	0.8085	0.7643	0.8418	0.8143	0.8457	0.8031

TABLE IV. CLASSIFICATION RESULTS OF CEEMDAN

Model	ACC	SEN	SPEC	PPV	NPV	AUROC
LGBM	0.8758	0.8464	0.9000	0.8829	0.8924	0.8732
XGB	0.8536	0.8179	0.8800	0.8417	0.8636	0.8489
GB	0.8320	0.8179	0.8436	0.8012	0.8592	0.8307
RF	0.8425	0.8264	0.8418	0.8020	0.8792	0.8441
SVM	0.8196	0.8179	0.8218	0.7817	0.8582	0.8198

The proposed ECEEMDAN-based framework produced the best overall results, with LGBM achieving the highest accuracy of 90.56% and an AUROC of 0.9120, along with strong sensitivity (92.10%) and specificity (90.23%), indicating superior discrimination of knee joint abnormalities. All performance metrics were evaluated using 10-fold stratified cross-validation. The proposed ECEEMDAN-LGBM framework achieved an average accuracy of 90.56±1.8%, an AUROC of 0.912±0.021, sensitivity 92.10±2.3%, and specificity 90.23±2.1% across folds, indicating stable performance. Statistical validation was performed using McNemar's test on paired predictions, confirming that the proposed ECEEMDAN-LGBM significantly outperforms EMD-, EEMD-, and CEEMDAN-based baselines as well as RF, XGB, and SVM classifiers (p = 0.012–0.039). The comparison with GB was not statistically significant (p = 0.062), with a 95% confidence interval of [83.0%, 95.0%].

TABLE V. CLASSIFICATION RESULTS OF ECEEMDAN

Model	ACC	SEN	SPEC	PPV	NPV	AUROC
LGBM	0.9056	0.9210	0.9023	0.8756	0.9395	0.9120
XGB	0.8542	0.8429	0.8618	0.8479	0.8871	0.8523
GB	0.8536	0.8429	0.8600	0.8364	0.8797	0.8514
RF	0.8529	0.8214	0.8800	0.8873	0.8910	0.8507
SVM	0.8418	0.8143	0.8618	0.8347	0.8757	0.8381

TABLE VI. STATISTICAL SIGNIFICANCE OF THE RESULTS

Reference model(s) compared with ECEEMDAN-LGBM	p-value range	Overall significance
EMD, EEMD, CEEMDAN, RF, XGB, SVM	0.012 – 0.039	Significant ($p < 0.05$)
GB	0.062	Not significant

The aggregated confusion matrix in Table VII demonstrates low false-negative and false-positive rates, confirming that the observed improvements are robust and not due to random variation.

TABLE VII. AGGREGATED CONFUSION MATRIX

Actual / Predicted	Normal	Abnormal
Normal (51)	46 (TN)	5 (FP)
Abnormal (38)	3 (FN)	35 (TP)

IV. DISCUSSION

This study used EMD variants, such as EMD, EEMD, CEEMDAN, and ECEEMDAN, to effectively decompose the VAG signal. These methods were used to determine the unwanted frequency components, i.e., the unwanted IMFs that can be discarded while reconstructing the signal. The remaining IMFs give precise representations of frequencies, which are essential for picking up and representing the abnormalities. The proposed method to identify significant IMFs is based on a weight-based mechanism that integrates energy, correlation, and kurtosis as key discriminative features. LGBM was employed not only as a classifier but also to assess the relative importance of these features. This facilitated the ranking of IMFs, and either the top-5 or those exceeding a dynamically defined threshold were retained for signal reconstruction.

The selected IMFs, along with reconstructed signals, were used in feature extraction, along with entropy features such as Approximate Entropy (ApEn), Sample Entropy (SampEn), and

Shannon Entropy (ShaEn). LGBM consistently demonstrated superior classification performance compared to SVM, RF, GB, DT, and XGB. This feature-guided IMF selection framework not only reduced noise, but also preserved diagnostically relevant components, improving overall classifier performance. These findings support the proposed ECEEMDAN-LGBM framework for non-invasive knee disorder assessment. Table V shows a comparison of the proposed method with existing ones that used the same dataset.

TABLE VIII. CLASSIFICATION RESULT COMPARISON

Study	Feature set employed	Classification approach	Accuracy (%)
[32]	OMPTFD-based energy and spectral parameters	Logistic Regression	68.90
[33]	Power spectral attributes	FLDA and Neural Network with RBF	74.00
[34]	Wavelet-derived features	LDA-based classification	79.80
[35]	CEEMDAN	Random Forest	86.61
[8]	TQWT	SVM	80.89
[22]	EWT-derived statistical parameters	SVM	83.33
[23]	TQWT and entropy	Ensemble	87.64
This work	Variants of EMDs and entropy features	LGBM	90.56

V. CONCLUSION

The study presented an effective and adaptive approach for the non-invasive detection of knee joint abnormalities using VAG signals. The proposed ECEEMDAN-LGBM framework addresses the major problems that are commonly noticed in EMD methods, such as mode mixing, noise interference, and inconsistent IMF selection, by combining advanced signal decomposition with intelligent feature-driven classification. This approach uses a novel IMF selection mechanism based on correlation, kurtosis, and energy thresholding to reconstruct signals. The feature set included entropy-based characteristics derived from the selected IMFs, along with the reconstructed signals.

The extracted features were classified using multiple machine learning classifiers, among which LGBM was consistently superior across all decomposition methods. In particular, the ECEEMDAN-LGBM framework achieved the highest accuracy of 90.56% and AUROC of 0.9120, demonstrating a strong sensitivity 92.10%, specificity of 90.23%, positive predictive value of 87.56%, and negative predictive value of 93.95%. These results indicate the potential of combining adaptive decomposition with ensemble learning methods for reliable, non-invasive diagnosis of knee pathologies. However, this study is limited by a modest sample size, the use of a single dataset, a lack of pathology subtype differentiation, and clinical validation. Future work will address these limitations through larger, multi-center datasets and clinical studies.

ACKNOWLEDGEMENT

The authors are grateful to the Indian government's Science and Engineering Research Board (SERB) for funding this study under grant no. CRG/2021/004501. The authors also are grateful to Prof. Rangaraj M. Rangayyan of the University of Calgary in Canada for providing the VAG dataset utilized in this investigation [4, 5].

REFERENCES

[1] R. Karpiński *et al.*, "Articular Cartilage: Structure, Biomechanics, and the Potential of Conventional and Advanced Diagnostics," *Applied Sciences*, vol. 15, no. 12, June 2025, Art. no. 6896, https://doi.org/10.3390/app15126896.

[2] A. C. Gelber, "Knee Osteoarthritis," *Annals of Internal Medicine*, vol. 177, no. 9, pp. ITC129–ITC144, Sept. 2024, https://doi.org/10.7326/ANNALS-24-01249.

[3] Ł. Bryliński *et al.*, "Trace Elements—Role in Joint Function and Impact on Joint Diseases," *International Journal of Molecular Sciences*, vol. 26, no. 15, Aug. 2025, Art. no. 7493, https://doi.org/10.3390/ijms26157493.

[4] R. M. Rangayyan, S. Krishnan, G. D. Bell, C. B. Frank, and K. O. Ladly, "Parametric representation and screening of knee joint vibroarthrographic signals," *IEEE Transactions on Biomedical Engineering*, vol. 44, no. 11, pp. 1068–1074, Nov. 1997, https://doi.org/10.1109/10.641334.

[5] S. Krishnan, R. M. Rangayyan, G. D. Bell, C. B. Frank, and K. O. Ladly, "Adaptive filtering, modelling and classification of knee joint vibroarthrographic signals for non-invasive diagnosis of articular cartilage pathology," *Medical & Biological Engineering & Computing*, vol. 35, no. 6, pp. 677–684, Nov. 1997, https://doi.org/10.1007/BF02510977.

[6] M. M. Shidore, S. S. Athreya, S. Deshpande, and R. Jalnekar, "Screening of knee-joint vibroarthrographic signals using time and spectral domain features," *Biomedical Signal Processing and Control*, vol. 68, July 2021, Art. no. 102808, https://doi.org/10.1016/j.bspc.2021.102808.

[7] Y. Wu *et al.*, "Quantification of knee vibroarthrographic signal irregularity associated with patellofemoral joint cartilage pathology based on entropy and envelope amplitude measures," *Computer Methods and Programs in Biomedicine*, vol. 130, pp. 1–12, July 2016, https://doi.org/10.1016/j.cmpb.2016.03.021.

[8] E. Mascarenhas, S. Nalband, A. R. J. Fredo, and A. A. Prince, "Analysis and Classification of Vibroarthrographic Signals using Tuneable 'Q' Wavelet Transform," in *2020 7th International Conference on Signal Processing and Integrated Networks (SPIN)*, Feb. 2020, pp. 65–70, https://doi.org/10.1109/SPIN48934.2020.9071335.

[9] Y. Athavale and S. Krishnan, "A telehealth system framework for assessing knee-joint conditions using vibroarthrographic signals," *Biomedical Signal Processing and Control*, vol. 55, Jan. 2020, Art. no. 101580, https://doi.org/10.1016/j.bspc.2019.101580.

[10] N. Befrui *et al.*, "Vibroarthrography for early detection of knee osteoarthritis using normalized frequency features," *Medical & Biological Engineering & Computing*, vol. 56, no. 8, pp. 1499–1514, Aug. 2018, https://doi.org/10.1007/s11517-018-1785-4.

[11] S. Gharehbaghi, D. C. Whittingslow, L. A. Ponder, S. Prahalad, and O. T. Inan, "Acoustic Emissions From Loaded and Unloaded Knees to Assess Joint Health in Patients With Juvenile Idiopathic Arthritis," *IEEE Journal of Biomedical and Health Informatics*, vol. 25, no. 9, pp. 3618–3626, Sept. 2021, https://doi.org/10.1109/JBHI.2021.3081429.

[12] R. E. Andersen, L. Arendt-Nielsen, and P. Madeleine, "Knee joint vibroarthrography of asymptomatic subjects during loaded flexion-extension movements," *Medical & Biological Engineering & Computing*, vol. 56, no. 12, pp. 2301–2312, Dec. 2018, https://doi.org/10.1007/s11517-018-1856-6.

[13] D. Moreira, J. Silva, M. V. Correia, and M. Massada, "Classification of knee arthropathy with accelerometer-based vibroarthrography," in *Studies in Health Technology and Informatics*, IOS Press, 2016.

[14] A. Łysiak, M. Szmajda, D. Bączkowicz, and D. Borzucka, "Transforming vibroarthrogram to the angle domain improves function–structure integration," *Biomedical Signal Processing and Control*, vol. 113, Mar. 2026, Art. no. 109112, https://doi.org/10.1016/j.bspc.2025.109112.

[15] A. Łysiak *et al.*, "Regression analysis of the vibroarthrogram in the external load conditions," *Advances in Science and Technology Research Journal*, vol. 19, no. 10, pp. 238–251, Oct. 2025, https://doi.org/10.12913/22998624/207975.

[16] R. Karpiński and A. Syta, "Application of encoder-based motion analysis and machine learning for knee osteoarthritis detection: A pilot study," *Applied Computer Science*, vol. 21, no. 4, pp. 21–31, Dec. 2025, https://doi.org/10.35784/acs_8410.

[17] R. Karpiński, "Knee Joint Osteoarthritis Diagnosis based on Selected Acoustic Signal Discriminants Using Machine :earning," *Applied Computer Science*, vol. 18, no. 2, pp. 71–85, June 2022, https://doi.org/10.35784/acs-2022-14.

[18] A. Machrowska, R. Karpiński, M. Maciejewski, J. Jonak, and P. Krakowski, "Application of EEMD-DFA Algorithms and ANN Classification for Detection of Knee Osteoarthritis Using Vibroarthrography," *Applied Computer Science*, vol. 20, no. 2, pp. 90–108, June 2024, https://doi.org/10.35784/acs-2024-18.

[19] R. Karpiński, P. Krakowski, J. Jonak, A. Machrowska, and M. Maciejewski, "Comparison of Selected Classification Methods Based on Machine Learning as a Diagnostic Tool for Knee Joint Cartilage Damage Based on Generated Vibroacoustic Processes," *Applied Computer Science*, vol. 19, no. 4, pp. 136–150, Dec. 2023, https://doi.org/10.35784/acs-2023-40.

[20] A. Machrowska, R. Karpiński, M. Maciejewski, J. Jonak, P. Krakowski, and A. Syta, "Application of Recurrence Quantification Analysis in the Detection of Osteoarthritis of the Knee with the Use of Vibroarthrography," *Advances in Science and Technology Research Journal*, vol. 18, no. 5, pp. 19–31, Sept. 2024, https://doi.org/10.12913/22998624/189512.

[21] K. Kręcisz, "Correlation between Linear and Non-Linear Vibroartrographic Parameters," *Przeglad Elektrotechniczny*, vol. 1, no. 7, pp. 182–187, July 2023, https://doi.org/10.15199/48.2023.07.33.

[22] K. S. Basavaraju, T. K. Kumar, K. A. Reddy, and K. R. K. Reddy, "Analysis of Vibroarthrographic signals for classification of knee disorders using Empirical Wavelet Transform based on Statistical measures," in *2023 IEEE International Instrumentation and Measurement Technology Conference (I2MTC)*, May 2023, pp. 1–6, https://doi.org/10.1109/I2MTC53148.2023.10175958.

[23] K. S. Basavaraju, T. K. Kumar, and K. A. Reddy, "Vibroarthrographic Signal Classification for Knee Joint Disorder Detection using Tunable Q-factor Wavelet Transform based on Entropy Measures," *Engineering, Technology & Applied Science Research*, vol. 15, no. 1, pp. 19953–19958, Feb. 2025, https://doi.org/10.48084/etasr.9245.

[24] S. Cai *et al.*, "Detrending knee joint vibration signals with a cascade moving average filter," in *2012 Annual International Conference of the IEEE Engineering in Medicine and Biology Society*, Aug. 2012, pp. 4357–4360, https://doi.org/10.1109/EMBC.2012.6346931.

[25] M. S. Calvo and H. S. Lee, "Enhanced COMPLETE ENSEMBLE EMD with superior noise handling capabilities: A robust signal decomposition method for power systems analysis," *Engineering Reports*, vol. 6, no. 11, Nov. 2024, Art. no. e12862, https://doi.org/10.1002/eng2.12862.

[26] N. E. Huang *et al.*, "The empirical mode decomposition and the Hilbert spectrum for nonlinear and non-stationary time series analysis," *Proceedings of the Royal Society of London. Series A: Mathematical, Physical and Engineering Sciences*, vol. 454, no. 1971, pp. 903–995, Mar. 1998, https://doi.org/10.1098/rspa.1998.0193.

[27] Z. Wu and N. E. Huang, "Ensemble Empirical Mode Decomposition: A Noise-Assisted Data Analysis Method," *Advances in Adaptive Data Analysis*, vol. 01, no. 01, pp. 1–41, Jan. 2009, https://doi.org/10.1142/S1793536909000047.

[28] M. A. Colominas, G. Schlotthauer, and M. E. Torres, "Improved complete ensemble EMD: A suitable tool for biomedical signal processing," *Biomedical Signal Processing and Control*, vol. 14, pp. 19–29, Nov. 2014, https://doi.org/10.1016/j.bspc.2014.06.009.

[29] S. M. Pincus, "Approximate entropy as a measure of system complexity.," *Proceedings of the National Academy of Sciences*, vol. 88, no. 6, pp. 2297–2301, Mar. 1991, https://doi.org/10.1073/pnas.88.6.2297.

[30] J. S. Richman and J. R. Moorman, "Physiological time-series analysis using approximate entropy and sample entropy," *American Journal of Physiology-Heart and Circulatory Physiology*, vol. 278, no. 6, pp. H2039–H2049, June 2000, https://doi.org/10.1152/ajpheart.2000.278.6.H2039.

[31] M. Ibl and J. Čapek, "Measure of Uncertainty in Process Models Using Stochastic Petri Nets and Shannon Entropy," *Entropy*, vol. 18, no. 1, Jan. 2016, Art. no. 33, https://doi.org/10.3390/e18010033.

[32] S. Krishnan, R. M. Rangayyan, G. D. Bell, and C. B. Frank, "Adaptive time-frequency analysis of knee joint vibroarthrographic signals for noninvasive screening of articular cartilage pathology," *IEEE Transactions on Biomedical Engineering*, vol. 47, no. 6, pp. 773–783, June 2000, https://doi.org/10.1109/10.844228.

[33] R. M. Rangayyan and Y. Wu, "Screening of knee-joint vibroarthrographic signals using probability density functions estimated with Parzen windows," *Biomedical Signal Processing and Control*, vol. 5, no. 1, pp. 53–58, Jan. 2010, https://doi.org/10.1016/j.bspc.2009.03.008.

[34] K. Umapathy and S. Krishnan, "Modified Local Discriminant Bases Algorithm and Its Application in Analysis of Human Knee Joint Vibration Signals," *IEEE Transactions on Biomedical Engineering*, vol. 53, no. 3, pp. 517–523, Mar. 2006, https://doi.org/10.1109/TBME.2005.869787.

[35] S. Nalband, A. Prince, and A. Agrawal, "Entropy-based feature extraction and classification of vibroarthographic signal using complete ensemble empirical mode decomposition with adaptive noise," *IET Science, Measurement & Technology*, vol. 12, no. 3, pp. 350–359, May 2018, https://doi.org/10.1049/iet-smt.2017.0284.